

Prion formation by a yeast GLFG nucleoporin

Randal Halfmann,^{1,3,t,||,*} Jessica R. Wright,^{4,5,t,||} Simon Alberti,^{1,5} Susan Lindquist^{1,3,*} and Michael Rexach^{4,*}

¹Whitehead Institute for Biomedical Research; Cambridge, MA USA; ²Department of Biology; Massachusetts Institute of Technology; Cambridge, MA USA;

³Howard Hughes Medical Institute; Massachusetts Institute of Technology; Cambridge, MA USA; ⁴MCD Biology Department; UC Santa Cruz; Santa Cruz, CA USA;

⁵Department of Biological Sciences; Stanford University; Stanford, CA USA

^tCurrent affiliations: Department of Biochemistry; UT Southwestern Medical Center; Dallas, TX USA; [†]Simons Foundation; New York, NY USA; [‡]Max Planck Institute of Molecular Cell Biology and Genetics; Dresden, Germany

^{||}These authors contributed equally to this work.

Keywords: nucleoporin, nuclear pore complex, yeast prion, GLFG nup, amyloid

Abbreviations: NPC, nuclear pore complex; nup, nucleoporin; FG nup, nup with Phe-Gly motif repeats; GLFG nup, nup with Gly-Leu-Phe-Gly motif repeats; AA, amino acid; PrD, prion forming domain; Sup35C, the C-terminal domain of Sup35; Nup100^{201–400}, AA 201–400 of Nup100; Nup100f, AA 300–400 of the Nup100 FG domain; WT, wild type; GdnHCl, guanidine hydrochloride

The self-assembly of proteins into higher order structures is both central to normal biology and a dominant force in disease. Certain glutamine/asparagine (Q/N)-rich proteins in the budding yeast *Saccharomyces cerevisiae* assemble into self-replicating amyloid-like protein polymers, or prions, that act as genetic elements in an entirely protein-based system of inheritance. The nuclear pore complex (NPC) contains multiple Q/N-rich proteins whose self-assembly has also been proposed to underlie structural and functional properties of the NPC. Here we show that an essential sequence feature of these proteins—repeating GLFG motifs—strongly promotes their self-assembly into amyloids with characteristics of prions. Furthermore, we demonstrate that Nup100 can form bona fide prions, thus establishing a previously undiscovered ability of yeast GLFG nucleoporins to adopt this conformational state in vivo.

Introduction

Prions are self-templating protein assemblies. Originally identified as agents of infectious neurological diseases,¹ prions are increasingly found to have diverse non-pathogenic roles. In the budding yeast, *Saccharomyces cerevisiae*, some proteins form prions with a wide range of phenotypic consequences, suggesting that these prions function to promote phenotypic diversity and expedite adaptive evolution.² For other proteins, prion formation may stem from a broader capacity for molecular self-recognition that underlies their normal cellular activities. In mammals, prion-like molecular switches propagate the antiviral innate immune response;³ in flies, they facilitate long-term memory formation.⁴

Prion formation is driven by modular and transferrable prion-forming domains (PrDs).^{5,6} Yeast PrDs are highly enriched for glutamines (Qs) and asparagines (Ns), but also contain well-spaced aromatic or hydrophobic residues.⁷ Together these features allow a prion protein to populate a “native” ensemble of soluble, disordered conformations.⁸ On rare occasion, the prion protein undergoes a dramatic conformational rearrangement to

produce a β -sheet-rich prion conformer, which then templates other soluble species to the same conformation. The result is a highly stable self-templating polymer or amyloid fibril, composed of individual prion-protein subunits.⁹

Prions can also stimulate other proteins to switch to their own prion states. The [RNQ⁺] prion, formed by the Q/N-rich protein Rnq1, cross-templates other Q/N-rich proteins. In at least one case, this activity is required for prion conversion de novo. Once formed, the new prions go on to propagate by themselves and no longer require [RNQ⁺].

Another factor, the protein disaggregase Hsp104, promotes prion formation in a different way. Hsp104 fragments amyloid fibers into small transmissible pieces that enable prions to be faithfully partitioned from mother cell to daughter over hundreds of cell divisions.^{10,11} This unique biochemical activity is critically required for the inheritance of most yeast prions.⁵

At least seven yeast proteins are known to form prions.^{5,12–14} An additional 18 proteins contain experimentally verified prion-forming domains (PrDs), and as many as 200 have sequence characteristics of prions.^{5,15} Among the latter are multiple subunits

*Correspondence to: Randal Halfmann, Susan Lindquist and Michael Rexach;
Emails: randal.halfmann@utsouthwestern.edu, lindquist_admin@wi.mit.edu and mrexach@ucsc.edu
Submitted: 02/22/12; Revised: 03/15/12; Accepted: 03/28/12
<http://dx.doi.org/10.4161/pri.20199>

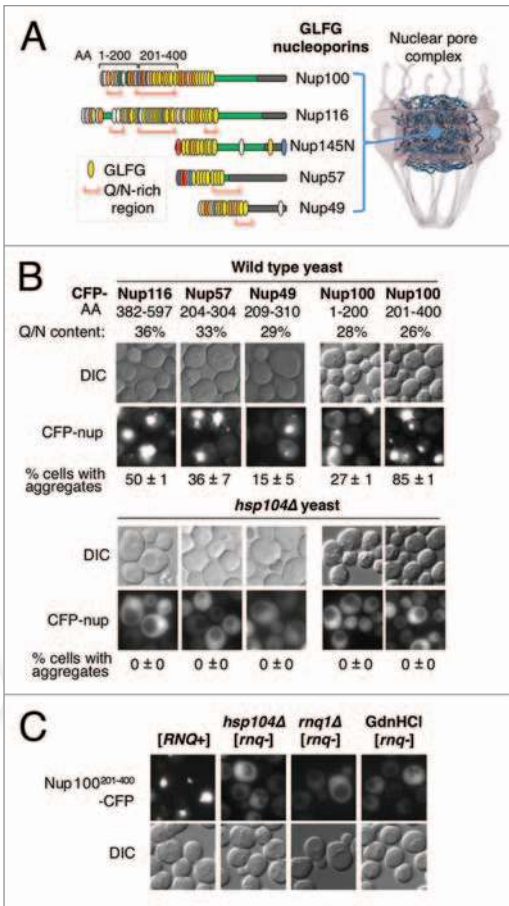


Figure 1. GLFG nucleoporins form prion-like aggregates. (A) Diagram of the NPC and of intrinsically-disordered GLFG nups populating its conduit. Each GLFG nup is shown as a green rectangle (N-terminus at left) and the location of FG motifs is indicated by vertical ovals. GLFG motifs are yellow, FxFG red, SPFG dark green, FxFx light gray, SAFG dark blue, PSFG bright green, NxFG light blue, SLFG orange, xxFG white and FxxFG lime green. The red brackets below each nup highlight the center of Q/N rich regions larger than 100 AA featuring $\geq 30\%$ Q/N content within 80 consecutive AAs. The horizontal gray rectangle in each nup marks its known or presumed NPC anchor domain.⁵⁷ (B) Intracellular aggregation of Q/N-rich regions of GLFG nups. Q/N-rich regions of Nup116, Nup57, Nup49 and Nup100 were overexpressed as CFP fusions in WT and *hsp104Δ* yeast from a constitutive ADH1 promoter. The percentage of cells ($n > 400$) with fluorescent Nup-CFP aggregates is indicated; standard deviation is from two independent experiments. (C) $[RNQ^+]$ -dependence of Nup100²⁰¹⁻⁴⁰⁰ aggregation. Nup100²⁰¹⁻⁴⁰⁰-CFP was overexpressed as in (B) in $[RNQ^+]$ cells and in cells converted to $[rnq^-]$ by deletion of *HSP104* (*hsp104Δ*); by deletion of *RNQ1* (*rnq1Δ*); or by treatment with 5 mM GdnHCl.

of the yeast nuclear pore complex (nups; NPC). The NPC is a supramolecular pore structure that gates all macromolecular exchange between the cytoplasm and nucleus.^{16,17} A subset of nups feature large intrinsically-disordered domains with numerous, repeated phenylalanine-glycine (FG) motifs that are interspersed with Q/N-rich segments (Fig. 1A).^{5,15,18-20} Hydrophobic interactions between FG motifs appear necessary to establish the NPC's size-selective protein diffusion barrier^{21,22} and to form

a central structural feature in the NPC conduit known as the transporter.^{23,24} FG motifs also serve as necessary docking sites for karyopherins as they shuttle across the NPC during nucleocytoplasmic trafficking.²⁵

Various FG nups can form hydrogels in vitro that recapitulate aspects of the NPC permeability barrier.^{21,26,27} These macroscopic hydrogels contain amyloid-like interactions between nups, suggesting a structural role for prion-like self-assembly mediated by the putative prion-forming domains of FG nups.²⁸ Whether nanoscopic amyloids or hydrogels also exist at the NPC remains to be seen.

We previously found that a subset of FG nups—those bearing glycine-leucine-phenylalanine-glycine (GLFG) repeats—formed two different types of cytosolic foci when overexpressed as fluorescent fusions without their NPC-tether domains. The biophysical properties of one type of foci, which we characterized in detail, suggested that they are structurally related to the NPC transporter.^{22,23} They formed in the absence of the prion-inducing factor $[RNQ^+]$ (i.e., in 5 mM guanidine-hydrochloride “cured” yeast) and were instantly and reversibly dispersed by exposure to 5% alcohols such as 1,6-hexanediol and ethanol.²² Thus, they were not amyloid/prion-like because amyloids are generally resistant to dispersion by alcohol. Moreover, while amyloid formation by most proteins is facilitated by $[RNQ^+]$,²⁹ non-amyloid foci typically form independently of $[RNQ^+]$.^{30,31} In contrast, when the same Q/N-rich GLFG domains were overexpressed in wild type yeast containing $[RNQ^+]$, they formed highly-stable, prion-like, amyloid aggregates.⁵ Here, we focus on the amyloid forming properties of these proteins and undertake a detailed investigation of the sequence features that govern amyloid, and indeed, prion formation by one GLFG nup in particular, Nup100.

Results

GLFG domains form prion-like aggregates. The *S. cerevisiae* GLFG nups contain one or more amino acid regions with a high density of Q/N residues similar to those found in yeast prion-forming proteins (Fig. 1A).^{5,15,18} To determine their capability for prion-like aggregation, we overexpressed the Q/N-rich regions in wild type $[RNQ^+]$ yeast as cyan-fluorescent protein (CFP)-fusions. All of them coalesced into bright cytoplasmic foci (Fig. 1B, top part). The region of Nup100 with the highest propensity to form foci Nup100²⁰¹⁻⁴⁰⁰ also contained a high Q/N content.

To determine if the observed nup aggregation required the prion partitioning factor Hsp104, the same nups were overexpressed in *hsp104Δ* cells. Foci did not form (Fig. 1B, bottom part). These cells also would have lacked the prion inducing factor $[RNQ^+]$, which requires Hsp104 for its presence. To test specifically for dependence on $[RNQ^+]$, we eliminated it by transiently disrupting Hsp104 activity with 5 mM guanidine hydrochloride (GdnHCl), a chemical inhibitor of Hsp104.^{32,33} We then re-examined the cells for nup aggregation upon restoration of Hsp104 activity. As shown here for Nup100²⁰¹⁻⁴⁰⁰ (Fig. 1C), the CFP-nup foci did not form in these cells, demonstrating their strong dependence on pre-existing $[RNQ^+]$. The nup fragments

used here (~100–200 AAs long) also did not form the alcohol-dispersible foci characterized by Patel et al. This was consistent with our demonstration that there is a nup size-dependent threshold (> 240 AA) for the formation of the alcohol-dispersible, NPC-like foci in yeast.²²

The faithful replication of prions in the crowded cellular milieu requires a high degree of sequence specificity. On the other hand, GLFG nups interact promiscuously with one another via their cohesive FG motifs.²² To examine the cellular effects of nup amyloids in the cytosol, we characterized the ability of Nup100^{201–400} aggregates to mislocalize other GLFG nups. First, we asked if the cytoplasmic foci containing overexpressed Nup100^{201–400} could recruit any of the yeast GLFG nups expressed from their endogenous loci. To track their localization, some were tagged with GFP via gene fusion at their chromosomal loci and their localization was examined by fluorescence microscopy. In the absence of Nup100^{201–400} overexpression, the GLFG nups were distributed exclusively around the nuclear rim (Fig. S1), as expected for components of the NPC. In contrast, when Nup100^{201–400} was overexpressed, the GLFG nups also mislocalized to cytoplasmic foci (Fig. 2A). Overexpression of Nup100^{201–400} caused Nup100-GFP to form foci in 30% of cells; Nup116-GFP to form foci in 13% of cells, and Nup49-GFP to form foci in 6% of cells. In contrast, the localization of Nup2-GFP, which lacks GLFG motifs and a Q/N-rich region, was unaffected by Nup100^{201–400} overexpression (Fig. 2A).

In a complementary analysis, Nup100^{201–400} was overexpressed in cells and the aggregation of untagged endogenous nups was assessed by their insolubility. Yeast lysates were separated into soluble (supernatant) and insoluble (pellet) fractions by centrifugation at 13,000x g. Proteins were then resolved by SDS-PAGE and processed by western blot analysis using anti-GLFG nup antibodies. As expected, endogenous GLFG nups and overexpressed Nup100^{201–400}-CFP were soluble in [*rnq*⁻] cell extracts. However, in [*RNQ*⁺] extracts they were also detected in the insoluble fraction together with overexpressed Nup100^{201–400}-CFP (Fig. 2B). Combined the results showed that endogenous GLFG nups can be recruited and mislocalized to cytosolic amyloids formed by an overexpressed GLFG domain.

A GLFG domain forms amyloids in vitro. A definitive biochemical characteristic of yeast prion proteins is an intrinsic capacity to form self-templating amyloids via nucleated conformational conversion.^{5,34} The region of Nup100 with the highest similarity to yeast prions is AA 300–400, which we designate as Nup100f. It has 38% Q/N residues and contains seven FG repeats (of mostly GLFG motifs) (Fig. 3A). To examine the amyloid-forming propensity of this Nup100 fragment in vitro, bacterially expressed His-tagged Nup100f was purified under denaturing conditions followed by dilution into a physiological buffer. Amyloid assembly was monitored using thioflavin-T (ThT), which is an amyloid-specific dye that changes fluorescence properties upon binding to amyloid structures, without affecting the kinetics of amyloid formation. After four hours of incubation under continuous agitation, ThT fluorescence began to increase

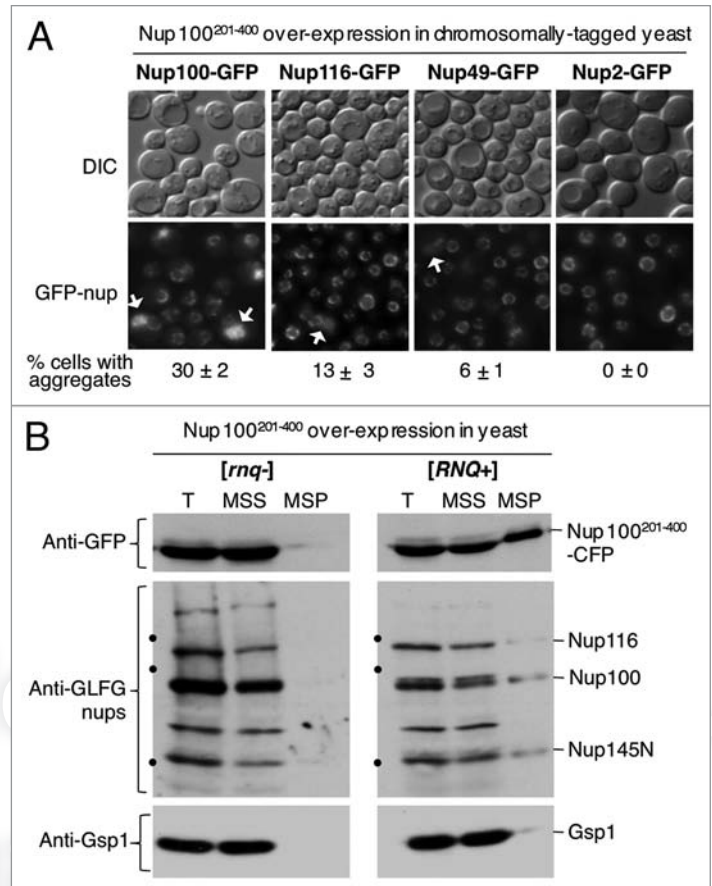


Figure 2. The prion-like region of Nup100 forms insoluble aggregates that sequester endogenous GLFG nups. (A) Mislocalization of endogenous nups by overexpressed Nup100^{201–400}. Yeast containing a chromosomal fusion of Nup100, Nup116, Nup49 or Nup2 with GFP were transformed with a plasmid that overexpresses Nup100^{201–400}. The percent of cells with cytoplasmic nup aggregates (n > 400) is shown below the pictures. Standard deviation (±) is from two independent experiments. The arrowheads point to cytoplasmic nup aggregates in cells, next to the more typical nuclear rim fluorescence pattern of the nup. (B) Aggregation of endogenous nups induced by overexpressed Nup100^{201–400}. [*rnq*⁻] and [*RNQ*⁺] cells overexpressing Nup100^{201–400}-CFP were lysed and cleared of unbroken cells by centrifugation at 2,000x g. The low speed supernatant fraction (T) was fractionated further at 12,000x g into medium speed supernatant (MSS) and pellet (MSP) fractions. Proteins in each fraction were resolved by SDS-PAGE, and the presence of Nup100^{201–400}-CFP, Gsp1 and endogenous GLFG nups were detected by western blotting with anti-GFP, anti-Gsp1 or anti-GLFG nup antibodies. The black dots on the gel frames mark the position of 116, 97 and 68 kDa molecular weight markers.

exponentially with kinetics similar to other well-characterized amyloid forming proteins (Fig. 3B, right part, no seeds).

Although de novo amyloid nucleation by prion proteins is slow, once formed amyloids can rapidly template the conformational conversion of additional soluble prion protein into the amyloid state.³⁴ In vivo, these properties allow prion proteins to exist either as soluble non-prion conformers, or as self-templating prion conformers. To determine if Nup100f amyloids have self-templating capacity, we added a small quantity of pre-assembled Nup100f amyloids (5% w/w) to de novo amyloid assembly reactions. Indeed, the lag phase to amyloid formation was eliminated

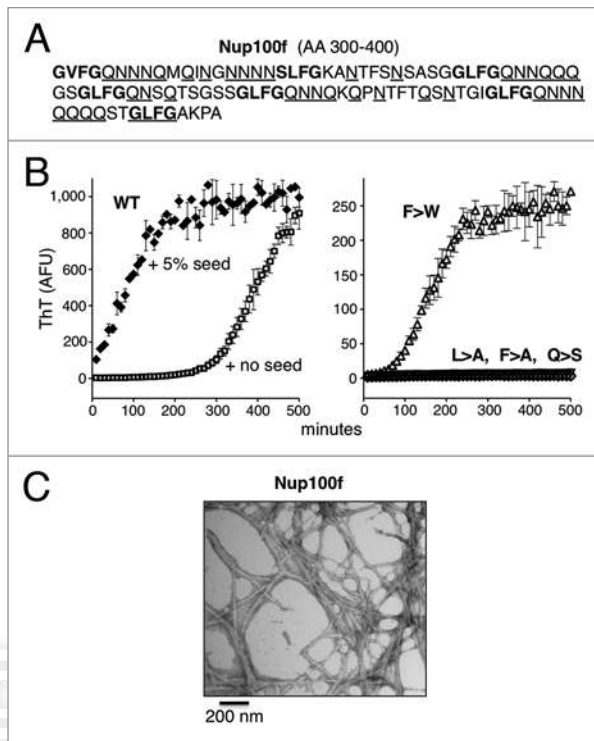


Figure 3. Nup100f forms amyloids under physiological conditions. (A) AA sequence of Nup100f. FG motifs are highlighted in bold text; Q/N residues are underlined. (B) Kinetics of Nup100f amyloid formation in vitro. Left part: Nup100f-*Trp-7xHis* (WT) was diluted from denaturant to 20 μ M in assembly buffer. The reaction was incubated at 30°C with agitation, in the absence or presence of 5% pre-formed aggregate seed. Amyloid assembly was monitored by ThT fluorescence. Data represent means \pm SEM from three reactions. Right part: The indicated Nup100f-*Trp-7xHis* variants were assembled in the absence of pre-formed fiber seeds. (C) Ultrastructure of WT Nup100f amyloids. Seeded amyloids formed as in (B) were negatively stained with uranyl acetate and examined by transmission electron microscope. Scale bar, 200 nm.

(Fig. 3B). When examined under the electron microscope, the Nup100f aggregates had classic fibrillar amyloid morphology (Fig. 3C), similar to other prions assembled in vitro.

To investigate the amyloid-forming properties of Nup100f in its normal context of a much larger GLFG domain, we utilized a region of the protein comprising AA 1–595, almost the entire GLFG domain (Fig. 1A). The protein was expressed, purified and analyzed under the same conditions used for Nup100f. As expected from previous observations,⁵ it too formed amyloids, although with substantially-delayed kinetics (>12 h; not shown) relative to the smaller fragment. The resulting Nup100^{1–595} amyloids effectively templated the polymerization of freshly diluted protein (Fig. S2).

GLFG motifs drive amyloid aggregation. Along with an enrichment for Q and N residues, prion domains feature additional AA sequence determinants that are required for efficient propagation in yeast.⁵ Recent evidence points to a role for aromatic and hydrophobic residues.^{7,35} The aggregation-prone domains of yeast FG nups do contain aromatic and hydrophobic residues in the form of GLFG motifs (Figs. 1B and 3A).²² To

identify sequence determinants that contribute to nup amyloid formation, we generated Nup100f variants with reduced Q/N-richness (all glutamines replaced with serine; Q > S) or with disrupted GLFG repeats (L > A, F > A or F > W substitutions). These were expressed, purified, and tested for amyloid formation under the same conditions used for WT Nup100f. Similarly to WT, the hydrophobic F > W mutant exhibited ThT fluorescence after a short lag phase (~4 h) (Fig. 3B, left part). In contrast, the onset of ThT fluorescence by the F > A, L > A and Q > S mutants was severely delayed and required lengthy incubations (> 12 h) to form amyloid (right part). We concluded that both the Q/N-richness and the presence of hydrophobic/aromatic residues in GLFG repeats contribute strongly to the amyloidogenicity of Nup100f.

Amyloid formation is a multistep process involving the association of disordered monomers into oligomers, the conversion of oligomers into amyloidogenic nuclei, and the templating of soluble protein onto those nuclei.^{11,34,36} The GLFG motifs could potentially exert their influence at any of these steps. To investigate the amyloid templating step specifically, we obtained amyloids of all of the purified Nup100f WT and variants, and used them to seed the polymerization of freshly-diluted proteins. Each readily polymerized off of amyloids of the same sequence (Fig. 3B, left part; Fig. S3). In the presence of preformed amyloids of different sequence, however, each variant behaved differently. Soluble proteins with intact GLFG motifs (WT) or with the F > W substitution were promiscuous—they readily polymerized onto amyloids formed by other variants. In contrast, soluble proteins with disrupted GLFG motifs (L > A and F > A) were more sequence-specific and only polymerized inefficiently onto heterotypic templates. The Q > S mutation had a more modest effect on heterotypic templating. Together, these data suggest that the GLFG repeats primarily influence the templating competency of the soluble protein species, rather than of the amyloids themselves, perhaps through hydrophobic attractions between the repeats of the soluble protein and those on the amyloid surface.

GLFG motifs drive prion formation. Next we asked if the amyloid-forming properties of Nup100f allow it to form self-perpetuating states in vivo. For this test we created a chimeric prion reporter consisting of Nup100f fused to the non-prion domain of Sup35, which carries out its translation termination function (Fig. 4A). Sequestration of this domain via prion-driven aggregation of Sup35 causes a nonsense-suppression phenotype detected by adenine prototrophy and by the emergence of white-colored colonies from previously red-colored yeast carrying a nonsense mutation in *ADE1*.¹⁰ When endogenous Sup35 was replaced with the Nup100f-Sup35C chimera, it recapitulated the heritable phenotypic switch associated with the WT Sup35 prion: cells from red colonies spontaneously gave rise to white colonies upon restreaking (Fig. 4B). Thus, following standard prion nomenclature we will refer to the state of the Nup100f-Sup35C chimera associated with the white phenotype as [*100F*⁺]; and the original, non-prion state as [*100f*].

The presence of [*RNQ*⁺] prions in cells stimulates other cellular proteins (such as Sup35) to form prions, but its presence becomes

unnecessary for their subsequent propagation. $[100F^+]$ showed similar characteristics. Its appearance required $[RNQ^+]$ (Fig. 4D), and when $[RNQ^+]$ was eliminated by deletion of the $RNQ1$ gene, the white phenotype persisted. This demonstrated the continued presence of $[100F^+]$, despite the absence of $[RNQ^+]$ (Fig. S4).

Next we examined the contributions of Q/N-richness and GLFG motifs to prion formation by Nup100f. $[RNQ^+]$ strains bearing the Nup100f-Sup35 chimeric constructs were plated directly onto adenine-deficient media to examine spontaneous switching to the $[100F^+]$ state. Wild-type and F > W chimeras converted to $[100F^+]$ at a high frequency, the L > A at a slightly-lower frequency, and the F > A and Q > S at a drastically-reduced frequency (Fig. 4B). As with other amyloid-based yeast prions, all of the $[100F^+]$ variants should require the continuous activity of Hsp104 for propagation. To test this, Hsp104 activity was transiently repressed by growing cells on 5 mM GdnHCl followed by restreaking on normal media. The resulting colonies were red in color (Fig. 4C, bottom row) indicating a loss of $[100F^+]$ chimeric prions. Some of the cured colonies had a darker shade of red than their parent colony prior to GdnHCl-treatment and $[100F^+]$ induction. This is due to the fact that Hsp104-inhibition also eliminates the prion-inducing factor $[RNQ^+]$, resulting in a loss of the low level, spontaneous prion induction events that gave some of the original yeast a pink color.

Yeast prion amyloids are resistant to solubilization by the anionic detergent SDS.⁵ Hence, we used semi-denaturing detergent-agarose gel electrophoresis (SDD-AGE),^{3,37} to determine whether the $[100F^+]$ states coincided with the presence of SDS-resistant amyloid forms of Nup100f-Sup35C chimeras in the cell lysates. In each case, representative Ade⁺ colonies displayed increased amyloid formation (Fig. 4D). The WT, L > A and F > W variants, but not the F > A and Q > S variants, also exhibited detectable aggregation even in $[100f]$ cells that were $[RNQ^+]$, consistent with their relative efficiencies of $[100F^+]$ formation in this background. We conclude that the aromatic residues within the repeated GLFG motif strongly promote prion formation by this fragment of Nup100.

Prion formation by endogenous Nup100. Can full-length nups also self-assemble into amyloids or prions? To investigate, we first examined the aggregation tendency of full-length Nup100 when overexpressed as an EGFP fusion. Fluorescence microscopy revealed that it formed multiple punctate foci in each cell (Fig. 5A). However, unlike smaller regions of Nup100 (Nup100²⁰¹⁻⁴⁰⁰ and Nup100f), the foci containing full-length Nup100 also formed in $[rnq]$ cells.

Next, we subjected these cells to SDD-AGE and detected Nup100-EGFP using an antibody to GFP. A large fraction of Nup100-EGFP partitioned to an SDS-resistant aggregate in $[RNQ^+]$ cells, while only a small amount did so in $[rnq]$ cells (Fig. 5B). Thus, the foci formed by overexpressed Nup100-EGFP (Fig. 5A) were of two different types. Those in $[RNQ^+]$ cells were composed of amyloids, whereas those in $[rnq]$ cells were not. Instead, the appearance of the latter was consistent with our previous report that overexpressed GLFG domains of nups (missing the NPC anchor domains) coalesce into alcohol-dispersible foci in cells lacking $[RNQ^+]$.²² Notably, the foci observed here

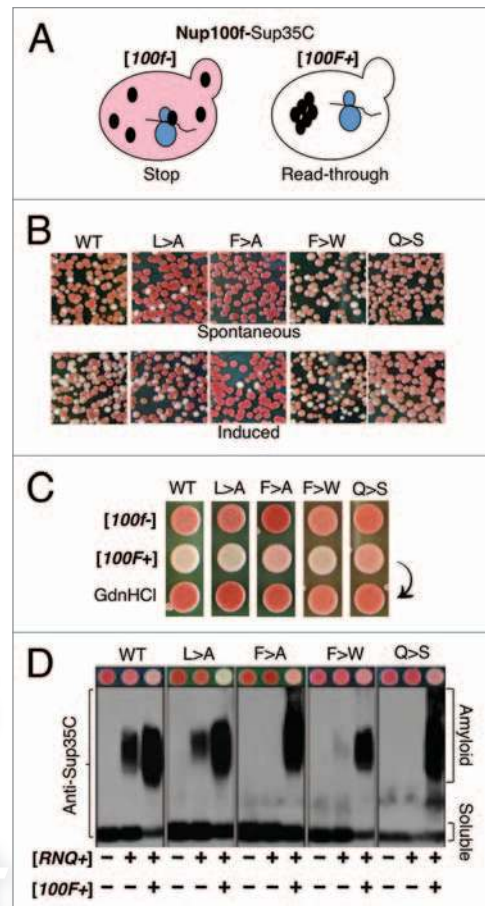


Figure 4. Nup100f is a prion-forming domain. (A) Schematic of the phenotypic reporter used to detect Nup100PrD-Sup35C prions. When WT Sup35 forms prion aggregates, it is sequestered away from its role in translation termination, causing a stop codon read-through phenotype that converts cells from red $[psi^-]$ to white $[PSI^+]$ (not shown). The Sup35PrD can be substituted for the Nup100PrD, resulting in a fully functional chimeric protein that recapitulates both the red ($[100f]$) and white ($[100F^+]$) states (shown). (B) Frequency of spontaneous and induced appearance of $[100F^+]$ in cells. WT or variant $[100f]$ $[RNQ^+]$ cells containing a galactose-inducible version of the respective Nup100f-EYFP were grown overnight in either glucose- or galactose-containing media, followed by plating to YPD to assess the appearance of white or pink $[100F^+]$ colonies. Red colonies derive from cells that remain $[100f]$. (C) Hsp104-dependence of $[100F^+]$ variants. WT and variant $[100f]$ strains were spotted onto YPD (top row). The corresponding $[100F^+]$ strains before and after GdnHCl treatment were spotted below. (D) Detection of SDS-resistant aggregates of Nup100f-Sup35C in lysates of prion-containing cells. Variant $[100f]$ and $[100F^+]$ cells in both $[rnq]$ and $[RNQ^+]$ strains were analyzed by SDD-AGE. The Nup100f-Sup35C fusion proteins were detected with anti-Sup35C antibodies. The color phenotype of the corresponding strains grown on YPD is shown above the SDD-AGE blots.

in $[rnq]$ cells could also reflect homotypic interactions between the C-terminal coiled-coil domain of Nup100, which normally tethers it to the NPC.

Next, we investigated whether the amyloids of Nup100-EGFP were capable of templating endogenous Nup100 into a self-sustaining amyloid state. We allowed $[RNQ^+]$ cells to overexpress Nup100-EGFP for hundreds of generations (five passages on

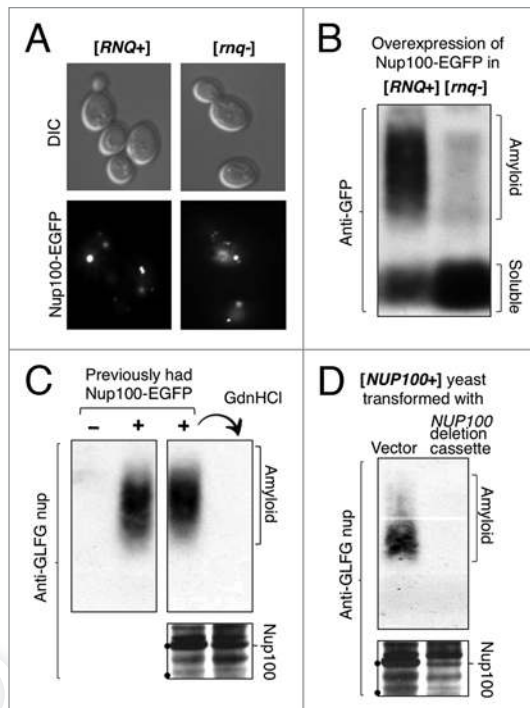


Figure 5. Prion-formation by full-length Nup100. (A) Overexpressed full-length Nup100-EGFP forms foci in both *[rnq-]* and *[RNQ+]* yeast. Cells containing NUP100-EGFP on a high copy galactose-inducible plasmid were grown overnight in galactose media, and then analyzed by fluorescence microscopy. (B) Detection of Nup100-EGFP amyloids in *[rnq-]* and *[RNQ+]* cell extracts. *[rnq-]* or *[RNQ+]* yeast expressing Nup100-EGFP as in (A) were analyzed by SDD-AGE. The blot was probed with anti-GFP, revealing SDS-resistant aggregates of Nup100-EGFP in *[RNQ+]* cells. (C) Prion formation by an endogenous GLFG nup. Cells that either had or had not overexpressed Nup100-EGFP, but no longer contained the Nup100-EGFP overexpression plasmid, were analyzed by SDD-AGE. Note how the transient overexpression of Nup100-EGFP induced persistent amyloids of endogenous GLFG nups, and these were eliminated by passage on GdnHCl. (D) GLFG nup prion amyloids require Nup100. *[NUP100+]* cells were transformed with either empty vector or a linearized *NUP100* gene-deletion cassette (targeted to create $\Delta nup100$). Verified transformants were analyzed by SDD-AGE as in (C). The black dots on the gel frames mark the position of 100 and 75 kDa molecular weight markers.

galactose-containing media), followed by growth on non-selective glucose media to allow loss of the Nup100-EGFP plasmid. Isolates that no longer contained the plasmid were then analyzed by SDD-AGE using an antibody against GLFG nups. Two of 12 such isolates now contained SDS-resistant high-molecular weight aggregates of the endogenous GLFG nups (one is shown in Fig. 5C). Isolates from lineages that had not overexpressed Nup100-EGFP did not contain such aggregates.

As cytoplasmic epigenetic elements, yeast prions do not follow the rules of classical nucleic acid inheritance, in which 50% of progeny inherit one parental trait and 50% the other. Instead prions are dominant in matings and typically segregate to all meiotic progeny. To test for prion-like inheritance patterns, we mated the GLFG nup amyloid-containing cells to a non-amyloid containing partner. The resulting diploids by SDD-AGE. The diploids contained GLFG nup amyloids (not shown). We then sporulated

these diploids to analyze inheritance patterns. The diploid lineages that we analyzed initially (generated from two independent amyloid-containing isolates) had very low spore viability. We did find, however, that the viable sporulants from these, when mated back to the original amyloid-free haploid, produced diploids that could themselves be sporulated to yield complete tetrads. These progeny were analyzed by SDD-AGE. Indeed, the presence of amyloids segregated in a non-Mendelian fashion. But rather than being inherited by 100% of sporulants, nup GLFG amyloids were found in only 12.5%: one sporulant in each of five tetrads and zero sporulants in another five tetrads (not shown). These sporadic inheritance patterns suggest that the GLFG nup amyloid trait is indeed caused by a prion, but one that becomes destabilized by the physiological changes accompanying sporulation.

As all known amyloid-based yeast prions require Hsp104, we temporarily inactivated Hsp104 by growing amyloid-containing cells on GdnHCl-containing media. We then re-analyzed the corresponding cell lysates by SDD-AGE, and observed that GdnHCl treatment eliminated the GLFG nup amyloids (Fig. 5C). When the cells were instead passaged on media lacking GdnHCl, the amyloids were retained. This demonstrated that GLFG nup amyloids are self-propagating, Hsp104-dependent assemblies.

To verify that the protein determinant of this novel prion state is indeed Nup100, we disrupted the genomic *NUP100* ORF in an amyloid-containing isolate using a drug-resistance cassette. In parallel, we transformed cells with an empty vector bearing the same cassette. We then examined lysates from both types of transformants by SDD-AGE. Cells containing an intact copy of *NUP100* still contained GLFG nup amyloids, while those containing a deletion of the *NUP100* gene did not (Fig. 5D). We conclude that the GLFG nucleoporin, Nup100, can be induced to form a prion in *S. cerevisiae*. In keeping with standard prion nomenclature, we designate its prion state as *[NUP100⁺]*.

What are the consequences of nucleoporin prions? Our early attempts to detect NPC-associated phenotypes in yeast containing cytosolic nup amyloids (induced by constitutive overexpression of Nup100²⁰¹⁻⁴⁰⁰) were largely unsuccessful. The yeast showed no significant growth or morphological defect, no defect in the NPC permeability barrier, no defect in Crm1-mediated export, no defect in mRNA export, and only a slight increase in the rate of nuclear import.³⁸ Given the functional redundancies of FG nups,³⁹ a lack of robust phenotypes for *[NUP100⁺]* would not be unexpected. Indeed, even genetic deletions of *NUP100* have few phenotypic consequences (www.yeastgenome.org). It remains to be seen if the promiscuity of GLFG interactions (Figs. 2 and S3) will enable *[NUP100⁺]* to stimulate other GLFG nups to switch to their own prion forms.

Discussion

The self-assembly of proteins has diverse cellular consequences. On the one hand, aberrant assemblies in the form of protein aggregates are often toxic and have driven the evolution of numerous protein folding quality-control mechanisms. On the other hand, a growing number of examples demonstrate that cells can also take advantage of protein aggregation.^{3,4,40,41}

Table 1. Yeast strains generated in this study

Name	Genotype and plasmotype	Construction
YSA329	MATa, leu2-3,112; his3-11,-15; trp1-1; ura3-1; ade1-14; can1-100; [RNQ ⁺]; sup35::HygB; pAG415ADH1-NUP100F-SUP35C	plasmid shuffle using YRS100 ⁵
YSA330	MATa, leu2-3,112; his3-11,-15; trp1-1; ura3-1; ade1-14; can1-100; [RNQ ⁺]; sup35::HygB; pAG415ADH1-NUP100F-SUP35C; [100F ⁺]	YSA329, Ade ⁺
YRH814	MATa, leu2-3,112; his3-11,-15; trp1-1; ura3-1; ade1-14; can1-100; [psi ⁻]; [RNQ ⁺]; pAG426Gal-NUP100-EGFP	transformation of YJW584 ⁴⁸
YRH821	MATa, leu2-3,112; his3-11,-15; trp1-1; ura3-1; ade1-14; can1-100; [psi ⁻]; [RNQ ⁺]; pAG426Gal-NUP100-EGFP; [NUP100 ⁺]	YRH814, grown on SGal-ura
YRH984	MATa, leu2-3,112; his3-11,-15; trp1-1; ura3-1; ade1-14; can1-100; [psi ⁻]; [RNQ ⁺]; [NUP100 ⁺]	YRH821, minus plasmid

In vitro, FG nups form self-assembling, gel-like matrices that have characteristics of amyloids;^{26,28} hence it was proposed that such amyloid-like structures are key elements of NPC function. Our findings here point to a different interpretation, namely, that FG domains in hydrogels reproduce the structure that FG domains adopt within cytosolic amyloids, rather than the structure they adopt natively at NPCs. This alternate hypothesis is based on two observations. First, the laboratory strains we examined here (derivatives of S288C, W303 and 74D-694) contained only trace amounts of putative GLFG nup amyloids as revealed by long exposures of SDD-AGE blots (not shown). In contrast, if the FG nups formed amyloid-like assemblies at the NPC, we would have expected them to be mostly SDS-insoluble. Second, given the extraordinary sensitivity of prion protein aggregation to the presence of pre-existing homotypic amyloids,^{42,43} one might have expected that overexpressed GLFG nups would readily form amyloids if the cells had naturally contained amyloids of the endogenous nups. Instead, overexpressed GLFG nups could only form amyloids in the presence of [RNQ⁺] prions, indicating that homotypic templates were not available in the cells. It remains possible, however, that GLFG nups at NPCs and in hydrogels form transient and highly localized amyloid-like interactions that may assist in their functions.²⁸

Nup amyloid formation was strongly promoted by GLFG motifs—the same AA sequence feature whose cohesive nature establishes the selective permeability barrier of the yeast NPC.^{22,39} Here we showed that the GLFG motifs greatly accelerated de novo amyloid formation as well as promiscuous recruitment of nups onto heterotypic templates, whereas the homotypic elongation of pre-existing amyloids was not noticeably affected by the motifs. Hence, the role of GLFG motifs in promoting amyloid formation could be fully explained by their previously-characterized cohesiveness. In the context of our experiments, the GLFG motif-driven interaction between nups likely promoted the formation of the oligomers that precede amyloid nucleation de novo. But in the confined geometry of the yeast NPC, such pre-amyloid interactions may rarely, if ever, mature into amyloid. This is because heterologous FG nups (up to 11 in *S. cerevisiae*) are confined to a limited space, stoichiometry and orientation.^{23,44}

The effect of GLFG repeats on amyloid and prion formation by Nup100 is consistent with the effect of aromatic and hydrophobic residues in other prion proteins. Aromatic-containing oligopeptide repeats occur frequently in prion proteins, including

Sup35, New1 and the mammalian prion PrP, and in all cases have been shown to increase the frequencies of prion formation.⁴⁵⁻⁴⁸ In the Sup35 prion domain, aromatics play a decisive role in the formation of oligomeric amyloid nuclei.⁴⁹ A recent comprehensive sequence analysis of yeast prions concluded that prion formation is directed by a compositional balance between aromatic/hydrophobic residues and disorder promoting residues like Q and N.⁷

Lastly, it is interesting that the repertoire of GLFG nups in yeast is 5-fold larger and much more Q/N-rich than that of humans, which only contain one type of GLFG nup (hNup98). Importantly however, even if human FG nups shared the tendency of its yeast counterparts to aggregate in vitro, human cells lack an Hsp104 homolog, which may be necessary for the efficient renaturation of aggregated proteins.⁵⁰ Hence, we posit that yeast have a unique capacity to exploit the aggregation tendencies of GLFG domains of nups in two ways. At the NPC, GLFG motif interactions are utilized to form a highly-effective sieve structure; whereas in the cytoplasm, they enable the formation of amyloids that can serve as benign, protein-based elements of inheritance.

Materials and Methods

Strains and plasmids. Yeast strain BY4741 was used in most analyses; derivatives of YRS100 were used for nonsense suppression assays.⁵ All these strains initially contained the prion element [RNQ⁺]. Strains generated for this work are listed in **Table 1**. Chromosomal integrations of GFP and deletions of *HSP104*, *RNQ1* and *NUP100* were accomplished by homologous recombination using PCR-based strategies.⁵¹⁻⁵⁴ Deletions were verified by diagnostic PCRs and immunoblots. Experiments in **Figures 1 and 2** utilized nup constructs cloned as CFP-fusions into pVT102-U, which allowed constitutive expression from an *ADHI*-promoter.^{22,55} Other experiments utilized Gateway plasmids. Stopless entry clones for *NUP100* and *NUP100F* were generated by PCR and recombination of the PCR products into pDONR221 as described previously in reference 5. Sequence-verified entry clones were then recombined into pAG415ADH-ccdB-SUP35C for heritable nonsense suppression assays; pAG424Gal-ccdB-EYFP for prion induction assays; pAG426Gal-ccdB-EGFP for aggregation analyses of full-length Nup100; and pRH1 for bacterial protein expression.^{5,56} Sequences of oligos and plasmids are available upon request.

Yeast procedures. Standard media and growth conditions were used throughout.⁵ For prion induction of Nup100f-Sup35C chimeras, cells were grown overnight in galactose-containing media prior to plating on glucose-containing media.

Microscopy. Yeast expressing fluorescent proteins were imaged live under a Nikon Eclipse 80i fluorescence microscope using a Nikon Plan Apo 100x/1.4 aperture objective. Photos were taken using a Hamamatsu Orca ER camera and Phylum Improvition software. For transmission electron microscopy, aggregates were negatively stained with uranyl acetate and imaged with a Phillips EM410 electron microscope.

Recombinant protein purification and amyloid assembly. Protein variants were expressed in *E. coli* BL21-A1 as Trp-7xHis fusions in pRH1 and purified as described previously in reference 5. Methanol-precipitated proteins were resuspended in 10–50 μ l of resuspension buffer (7 M GdnHCl; 100 mM K₂HPO₄, pH 5.0; 300 mM NaCl, 5 mM EDTA, 5 mM TCEP). Protein concentrations were determined by measuring absorption at 280 nm using calculated extinction coefficients. Protein stocks were heated for 5 min at 95°C before being diluted to 20 μ M in assembly buffer (5 mM K₂HPO₄, pH 6.6; 150 mM NaCl; 5 mM EDTA; 2 mM TCEP) plus 0.5 mM ThT. Seeded ThT reactions included up to 10% (w/w) fibers of pre-assembled proteins that were pre-sonicated for 10 sec with probe at setting 1 on a Branson Sonifier 250 sonicator. Assembly reactions (100 μ l) were performed in black nonbinding microplates (Corning, 3650), with medium orbital-shaking at 30°C on a Tecan Sapphire II plate reader. Fluorescence measurements were taken at 450 nm excitation, 482 nm emission.

SDD-AGE. Samples were lysed and processed as described previously in reference 5. A modified lysis buffer was used for the detection of endogenous Nup100, consisting of 100 mM TRIS-HCl pH 8, 20 mM NaCl, 2 mM MgCl₂, 50 mM

β -mercapto-ethanol, 1% Triton X-100, 2% Halt protease inhibitor cocktail (Thermo Scientific, 87785), 30 mM N-ethylmaleimide and 100 U/ml Benzonase (EMD, 70746). Washed cell pellets were lysed by glass-bead disruption followed by removal of cell-debris by centrifugation at 2,000 rcf for 2 min. Supernatants were combined with Laemmli sample buffer to achieve a concentration of 2% SDS and incubated for 5 min at room temperature prior to loading on 1.5% agarose gels containing 0.1% SDS. For **Figure 5B**, cultures were grown overnight in glucose-containing media and then washed and resuspended in galactose-containing media for 24 h to induce the expression of Nup100-EGFP prior to cell lysis. Note that although SDD-AGE reliably detects SDS-resistant aggregates, it does not reliably detect SDS-soluble protein species.³⁰ This resulted in our inability to detect non-amyloid forms of endogenous GLFG nups by SDD-AGE (e.g., **Fig. 5C**).

Disclosure of Potential Conflicts of Interest

No potential conflicts of interest were disclosed.

Acknowledgments

This work was supported by the G. Harold and Leila Y. Mathers Charitable Foundation. NIH grants GM061900 and GM007520 awarded to M.R., NIH grant GM25874 awarded to S.L., and an NIH Director's Early Independence Award, grant DP5-OD009152-01, awarded to R.H. S.L. is an investigator of the Howard Hughes Medical Institute. R.H. is a Frank and Sara McKnight Fellow at UTSWMC. We thank members of the Lindquist and Rexach labs for critical reading of the manuscript, and Jijun Dong for assistance with electron microscopy.

Supplemental Material

Supplemental materials may be found here: www.landesbioscience.com/journals/prion/article/20199

References

1. Prusiner SB. Novel proteinaceous infectious particles cause scrapie. *Science* 1982; 216:136-44; PMID:6801762; <http://dx.doi.org/10.1126/science.6801762>.
2. Halfmann R, Lindquist S. Epigenetics in the extreme: prions and the inheritance of environmentally acquired traits. *Science* 2010; 330:629-32; PMID:21030648; <http://dx.doi.org/10.1126/science.1191081>.
3. Hou F, Sun L, Zheng H, Skaug B, Jiang QX, Chen ZJ. MAVS forms functional prion-like aggregates to activate and propagate antiviral innate immune response. *Cell* 2011; 146:448-61; PMID:21782231; <http://dx.doi.org/10.1016/j.cell.2011.06.041>.
4. Majumdar A, Cesario WC, White-Grindley E, Jiang H, Ren F, Khan MR, et al. Critical role of amyloid-like oligomers of *Drosophila* Orb2 in the persistence of memory. *Cell* 2012; 148:515-29; PMID:22284910; <http://dx.doi.org/10.1016/j.cell.2012.01.004>.
5. Alberti S, Halfmann R, King O, Kapila A, Lindquist S. A systematic survey identifies prions and illuminates sequence features of prionogenic proteins. *Cell* 2009; 137:146-58; PMID:19345193; <http://dx.doi.org/10.1016/j.cell.2009.02.044>.
6. Li L, Lindquist S. Creating a protein-based element of inheritance. *Science* 2000; 287:661-4; PMID:10650001; <http://dx.doi.org/10.1126/science.287.5453.661>.
7. Toombs JA, McCarty BR, Ross ED. Compositional determinants of prion formation in yeast. *Mol Cell Biol* 2010; 30:319-32; PMID:19884345; <http://dx.doi.org/10.1128/MCB.01140-09>.
8. Mukhopadhyay S, Krishnan R, Lemke EA, Lindquist S, Deniz AA. A natively unfolded yeast prion monomer adopts an ensemble of collapsed and rapidly fluctuating structures. *Proc Natl Acad Sci USA* 2007; 104:2649-54; PMID:17299036; <http://dx.doi.org/10.1073/pnas.0611503104>.
9. Patino MM, Liu JJ, Glover JR, Lindquist S. Support for the prion hypothesis for inheritance of a phenotypic trait in yeast. *Science* 1996; 273:622-6; PMID:8662547; <http://dx.doi.org/10.1126/science.273.5275.622>.
10. Chernoff YO, Lindquist SL, Ono B, Inge-Vechtomov SG, Liebman SW. Role of the chaperone protein Hsp104 in propagation of the yeast prion-like factor [psi⁺]-[psi⁻]. *Science* 1995; 268:880-4; PMID:7754373; <http://dx.doi.org/10.1126/science.7754373>.
11. Shorter J, Lindquist S. Hsp104 catalyzes formation and elimination of self-replicating Sup35 prion conformers. *Science* 2004; 304:1793-7; PMID:15155912; <http://dx.doi.org/10.1126/science.1098007>.
12. Rogoza T, Goginashvili A, Rodionova S, Ivanov M, Viktorovskaya O, Rubel A, et al. Non-Mendelian determinant [ISP⁺] in yeast is a nuclear-residing prion form of the global transcriptional regulator Sfp1. *Proc Natl Acad Sci USA* 2010; 107:10573-7; PMID:20498075; <http://dx.doi.org/10.1073/pnas.1005949107>.
13. Patel BK, Gavin-Smyth J, Liebman SW. The yeast global transcriptional co-repressor protein Cyc8 can propagate as a prion. *Nat Cell Biol* 2009; 11:344-9; PMID:19219034; <http://dx.doi.org/10.1038/ncb1843>.
14. Du Z, Park KW, Yu H, Fan Q, Li L. Newly identified prion linked to the chromatin-remodeling factor Swi1 in *Saccharomyces cerevisiae*. *Nat Genet* 2008; 40:460-5; PMID:18362884; <http://dx.doi.org/10.1038/ng.112>.
15. Michelitsch MD, Weissman JS. A census of glutamine/asparagine-rich regions: implications for their conserved function and the prediction of novel prions. *Proc Natl Acad Sci USA* 2000; 97:11910-5; PMID:11050225; <http://dx.doi.org/10.1073/pnas.97.22.11910>.
16. Wentz SR, Rout MP. The nuclear pore complex and nuclear transport. *Cold Spring Harb Perspect Biol* 2010; 2:562; PMID:20630994; <http://dx.doi.org/10.1101/cshperspect.a000562>.
17. Hoelz A, Debler EW, Blobel G. The structure of the nuclear pore complex. *Annu Rev Biochem* 2011; 80:613-43; PMID:21495847; <http://dx.doi.org/10.1146/annurev-biochem-060109-151030>.
18. Wentz SR, Rout MP, Blobel G. A new family of yeast nuclear pore complex proteins. *J Cell Biol* 1992; 119:705-23; PMID:1385442; <http://dx.doi.org/10.1083/jcb.119.4.705>.
19. Denning DP, Patel SS, Uversky V, Fink AL, Rexach M. Disorder in the nuclear pore complex: the FG repeat regions of nucleoporins are natively unfolded. *Proc Natl Acad Sci USA* 2003; 100:2450-5; PMID:12604785; <http://dx.doi.org/10.1073/pnas.0437902100>.

20. DeGrasse JA, DuBois KN, Devos D, Siegel TN, Sali A, Field MC, et al. Evidence for a shared nuclear pore complex architecture that is conserved from the last common eukaryotic ancestor. *Mol Cell Proteomics* 2009; 8:2119-30; PMID:19525551; <http://dx.doi.org/10.1074/mcp.M900038-MCP200>.
21. Frey S, Görlich D. FG/FxFG as well as GLFG repeats form a selective permeability barrier with self-healing properties. *EMBO J* 2009; 28:2554-67; PMID:19680227; <http://dx.doi.org/10.1038/emboj.2009.199>.
22. Patel SS, Belmont BJ, Sante JM, Rexach MF. Natively unfolded nucleoporins gate protein diffusion across the nuclear pore complex. *Cell* 2007; 129:83-96; PMID:17418788; <http://dx.doi.org/10.1016/j.cell.2007.01.044>.
23. Yamada J, Phillips JL, Patel S, Goldfien G, Calestagne-Morelli A, Huang H, et al. A bimodal distribution of two distinct categories of intrinsically disordered structures with separate functions in FG nucleoporins. *Mol Cell Proteomics* 2010; 9:2205-24; PMID:20368288; <http://dx.doi.org/10.1074/mcp.M000035-MCP201>.
24. Akey CW. The NPC-transporter, a ghost in the machine. *Structure* 2010; 18:1230-2; PMID:20947011; <http://dx.doi.org/10.1016/j.str.2010.09.005>.
25. Terry LJ, Wentz SR. Flexible gates: dynamic topologies and functions for FG nucleoporins in nucleocytoplasmic transport. *Eukaryot Cell* 2009; 8:1814-27; PMID:19801417; <http://dx.doi.org/10.1128/EC.00225-09>.
26. Frey S, Görlich D. A saturated FG-repeat hydrogel can reproduce the permeability properties of nuclear pore complexes. *Cell* 2007; 130:512-23; PMID:17693259; <http://dx.doi.org/10.1016/j.cell.2007.06.024>.
27. Milles S, Lemke EA. Single molecule study of the intrinsically disordered FG-repeat nucleoporin 153. *Biophys J* 2011; 101:1710-9; PMID:21961597; <http://dx.doi.org/10.1016/j.bpj.2011.08.025>.
28. Ader C, Frey S, Maas W, Schmidt HB, Görlich D, Baldus M. Amyloid-like interactions within nucleoporin FG hydrogels. *Proc Natl Acad Sci USA* 2010; 107:6281-5; PMID:20304795; <http://dx.doi.org/10.1073/pnas.0910163107>.
29. Bradley ME, Edskes HK, Hong JY, Wickner RB, Liebman SW. Interactions among prions and prion "strains" in yeast. *Proc Natl Acad Sci USA* 2002; 99:16392-9; PMID:12149514; <http://dx.doi.org/10.1073/pnas.152330699>.
30. Douglas PM, Treusch S, Ren HY, Halfmann R, Duennwald ML, Lindquist S, et al. Chaperone-dependent amyloid assembly protects cells from prion toxicity. *Proc Natl Acad Sci USA* 2008; 105:7206-11; PMID:18480252; <http://dx.doi.org/10.1073/pnas.0802593105>.
31. Johnson BS, McCaffery JM, Lindquist S, Gitler AD. A yeast TDP-43 proteinopathy model: Exploring the molecular determinants of TDP-43 aggregation and cellular toxicity. *Proc Natl Acad Sci USA* 2008; 105:6439-44; PMID:18434538; <http://dx.doi.org/10.1073/pnas.0802082105>.
32. Ferreira PC, Ness F, Edwards SR, Cox BS, Tuite MF. The elimination of the yeast [PSI⁺] prion by guanidine hydrochloride is the result of Hsp104 inactivation. *Mol Microbiol* 2001; 40:1357-69; PMID:11442834; <http://dx.doi.org/10.1046/j.1365-2958.2001.02478.x>.
33. Grimminger V, Richter K, Imhof A, Buchner J, Walter S. The prion curing agent guanidinium chloride specifically inhibits ATP hydrolysis by Hsp104. *J Biol Chem* 2004; 279:7378-83; PMID:14668331; <http://dx.doi.org/10.1074/jbc.M312403200>.
34. Serio TR, Cshikar AG, Kowal AS, Sawicki GJ, Moslehi JJ, Serpell L, et al. Nucleated conformational conversion and the replication of conformational information by a prion determinant. *Science* 2000; 289:1317-21; PMID:10958771; <http://dx.doi.org/10.1126/science.289.5483.1317>.
35. Alexandrov IM, Vishnevskaya AB, Ter-Avanesyan MD, Kushnirov VV. Appearance and propagation of polyglutamine-based amyloids in yeast: tyrosine residues enable polymer fragmentation. *J Biol Chem* 2008; 283:15185-92; PMID:18381282; <http://dx.doi.org/10.1074/jbc.M802071200>.
36. Kodali R, Wetzel R. Polymorphism in the intermediates and products of amyloid assembly. *Curr Opin Struct Biol* 2007; 17:48-57; PMID:17251001; <http://dx.doi.org/10.1016/j.sbi.2007.01.007>.
37. Kryndushkin DS, Alexandrov IM, Ter-Avanesyan MD, Kushnirov VV. Yeast [PSI⁺] prion aggregates are formed by small Sup35 polymers fragmented by Hsp104. *J Biol Chem* 2003; 278:49636-43; PMID:14507919; <http://dx.doi.org/10.1074/jbc.M307996200>.
38. Wright JR. A family of yeast nucleoporins form novel prions. Palo Alto, CA: Stanford University 2006.
39. Strawn LA, Shen T, Shulga N, Goldfarb DS, Wentz SR. Minimal nuclear pore complexes define FG repeat domains essential for transport. *Nat Cell Biol* 2004; 6:197-206; PMID:15039779; <http://dx.doi.org/10.1038/ncb1097>.
40. Fowler DM, Koulov AV, Balch WE, Kelly JW. Functional amyloid—from bacteria to humans. *Trends Biochem Sci* 2007; 32:217-24; PMID:17412596; <http://dx.doi.org/10.1016/j.tibs.2007.03.003>.
41. Maji SK, Perrin MH, Sawaya MR, Jessberger S, Vadodaria K, Rissman RA, et al. Functional amyloids as natural storage of peptide hormones in pituitary secretory granules. *Science* 2009; 325:328-32; PMID:19541956; <http://dx.doi.org/10.1126/science.1173155>.
42. Santoso A, Chien P, Osherovich LZ, Weissman JS. Molecular basis of a yeast prion species barrier. *Cell* 2000; 100:277-88; PMID:10660050; [http://dx.doi.org/10.1016/S0092-8674\(00\)81565-2](http://dx.doi.org/10.1016/S0092-8674(00)81565-2).
43. Bruce KL, Chernoff YO. Sequence specificity and fidelity of prion transmission in yeast. *Semin Cell Dev Biol* 2011; 22:444-51; PMID:21439395; <http://dx.doi.org/10.1016/j.semdb.2011.03.005>.
44. Alber F, Dokudovskaya S, Veenhoff LM, Zhang W, Kipper J, Devos D, et al. The molecular architecture of the nuclear pore complex. *Nature* 2007; 450:695-701; PMID:18046406; <http://dx.doi.org/10.1038/nature06405>.
45. Tank EM, Harris DA, Desai AA, True HL. Prion protein repeat expansion results in increased aggregation and reveals phenotypic variability. *Mol Cell Biol* 2007; 27:5445-55; PMID:17548473; <http://dx.doi.org/10.1128/MCB.02127-06>.
46. Liu JJ, Lindquist S. Oligopeptide-repeat expansions modulate 'protein-only' inheritance in yeast. *Nature* 1999; 400:573-6; PMID:10448860; <http://dx.doi.org/10.1038/22919>.
47. Dong J, Bloom JD, Goncharov V, Chattopadhyay M, Millhauser GL, Lynn DG, et al. Probing the role of PrP repeats in conformational conversion and amyloid assembly of chimeric yeast prions. *J Biol Chem* 2007; 282:34204-12; PMID:17893150; <http://dx.doi.org/10.1074/jbc.M704952200>.
48. Osherovich LZ, Cox BS, Tuite MF, Weissman JS. Dissection and design of yeast prions. *PLoS Biol* 2004; 2:86; PMID:15045026; <http://dx.doi.org/10.1371/journal.pbio.0020086>.
49. Ohhashi Y, Ito K, Toyama BH, Weissman JS, Tanaka M. Differences in prion strain conformations result from non-native interactions in a nucleus. *Nat Chem Biol* 2010; 6:225-30; PMID:20081853; <http://dx.doi.org/10.1038/nchembio.306>.
50. Vashist S, Cushman M, Shorter J. Applying Hsp104 to protein-misfolding disorders. *Biochem Cell Biol* 2010; 88:1-13; PMID:20130674; <http://dx.doi.org/10.1139/O09-121>.
51. Wach A, Brachat A, Alberti-Segui C, Rebischung C, Philippens P. Heterologous HIS3 marker and GFP reporter modules for PCR-targeting in *Saccharomyces cerevisiae*. *Yeast* 1997; 13:1065-75; PMID:9290211; [http://dx.doi.org/10.1002/\(SICI\)1097-0061\(19970915\)13:11<1065::AID-YEA159>3.0.CO;2-K](http://dx.doi.org/10.1002/(SICI)1097-0061(19970915)13:11<1065::AID-YEA159>3.0.CO;2-K).
52. Longtine MS, McKenzie A, 3rd, Demarini DJ, Shah NG, Wach A, Brachat A, et al. Additional modules for versatile and economical PCR-based gene deletion and modification in *Saccharomyces cerevisiae*. *Yeast* 1998; 14:953-61; PMID:9717241; [http://dx.doi.org/10.1002/\(SICI\)1097-0061\(199807\)14:10<953::AID-YEA293>3.0.CO;2-U](http://dx.doi.org/10.1002/(SICI)1097-0061(199807)14:10<953::AID-YEA293>3.0.CO;2-U).
53. Baudin A, Ozier-Kalogeropoulos O, Denouel A, Lacroute F, Cullin C. A simple and efficient method for direct gene deletion in *Saccharomyces cerevisiae*. *Nucleic Acids Res* 1993; 21:3329-30; PMID:8341614; <http://dx.doi.org/10.1093/nar/21.14.3329>.
54. Goldstein AL, McCusker JH. Three new dominant drug resistance cassettes for gene disruption in *Saccharomyces cerevisiae*. *Yeast* 1999; 15:1541-53; PMID:10514571; [http://dx.doi.org/10.1002/\(SICI\)1097-0061\(199910\)15:14<1541::AID-YEA476>3.0.CO;2-K](http://dx.doi.org/10.1002/(SICI)1097-0061(199910)15:14<1541::AID-YEA476>3.0.CO;2-K).
55. Vernet T, Dignard D, Thomas DY. A family of yeast expression vectors containing the phage fl intergenic region. *Gene* 1987; 52:225-33; PMID:3038686; [http://dx.doi.org/10.1016/0378-1119\(87\)90049-7](http://dx.doi.org/10.1016/0378-1119(87)90049-7).
56. Alberti S, Gitler AD, Lindquist S. A suite of Gateway cloning vectors for high-throughput genetic analysis in *Saccharomyces cerevisiae*. *Yeast* 2007; 24:913-9; PMID:17583893; <http://dx.doi.org/10.1002/yea.1502>.
57. Denning DP, Rexach MF. Rapid evolution exposes the boundaries of domain structure and function in natively unfolded FG nucleoporins. *Mol Cell Proteomics* 2007; 6:272-82; PMID:17079785; <http://dx.doi.org/10.1074/mcp.M600309-MCP200>.